

UCLA

UCLA Previously Published Works

Title

Investigating PSMA-Targeted Radioligand Therapy Efficacy as a Function of Cellular PSMA Levels and Intratumoral PSMA Heterogeneity

Permalink

<https://escholarship.org/uc/item/8wm354nr>

Journal

Clinical Cancer Research, 26(12)

ISSN

1078-0432

Authors

Current, Kyle
Meyer, Catherine
Magyar, Clara E
et al.

Publication Date

2020-06-15

DOI

10.1158/1078-0432.ccr-19-1485

Peer reviewed



Published in final edited form as:

Clin Cancer Res. 2020 June 15; 26(12): 2946–2955. doi:10.1158/1078-0432.CCR-19-1485.

Investigating PSMA-targeted radioligand therapy efficacy as a function of cellular PSMA levels and intra-tumoral PSMA heterogeneity

Kyle Current¹, Catherine Meyer¹, Clara Magyar², Christine E. Mona¹, Joel Almajano¹, Roger Slavik¹, Andreea D. Stuparu¹, Chloe Cheng¹, David W. Dawson², Caius G. Radu¹, Johannes Czernin¹, Katharina Lückerath^{1,*}

¹Department of Molecular and Medical Pharmacology, David Geffen School of Medicine at University of California, Los Angeles (UCLA), CA, USA

²Department of Pathology and Laboratory Medicine, David Geffen School of Medicine at University of California, Los Angeles (UCLA), CA, USA

Abstract

Purpose: Prostate specific membrane antigen (PSMA) targeting radioligands deliver radiation to PSMA expressing cells. However, the relationship between PSMA levels and intra-lesion heterogeneity of PSMA expression, and cytotoxic radiation by radioligand therapy (RLT) is unknown. Here we investigate RLT efficacy as function of PSMA levels/cell, and the fraction of PSMA-positive cells in a tumor.

Experimental design: RM1 cells expressing different levels of PSMA (PSMA⁻, PSMA⁺, PSMA⁺⁺, PSMA⁺⁺⁺; study 1) or a mix of PSMA-positive and -negative RM1 (study 2, 4) or PC-3/PC-3-PIP (study 3) cells at various ratios were injected into mice. Mice received ¹⁷⁷Lu- (studies 1–3) or ²²⁵Ac- (study 4) PSMA617. Tumor growth was monitored. Two days post-RLT, tumors were resected in a subset of mice. Radioligand uptake and DNA damage were quantified.

Results: ¹⁷⁷Lu-PSMA617 efficacy increased with increasing PSMA levels (study 1) and fractions of PSMA positive cells (studies 2, 3) in both, the RM1 and PC-3-PIP models. In tumors resected two days post-RLT, PSMA expression correlated with ¹⁷⁷Lu-PSMA617 uptake and the degree of DNA damage. Compared to ¹⁷⁷Lu-PSMA617, ²²⁵Ac-PSMA617 improved overall anti-tumor effectiveness and tended to enhance the differences in therapeutic efficacy between experimental groups.

Conclusion: In the current models both the degree of PSMA expression and the fraction of PSMA-positive cells correlate with ¹⁷⁷Lu-/²²⁵Ac-PSMA617 tumor uptake and DNA damage, and thus, RLT efficacy. Low or heterogeneous PSMA expression represents a resistance mechanism to RLT.

*Correspondence to: Katharina Lückerath, University of California, Los Angeles, Ahmanson Translational Imaging Division, 650 Charles E Young Drive South, Los Angeles, CA 90095-7370, klueckerath@mednet.ucla.edu.

Disclosure of potential conflicts of interest. JC and CR are co-founders and hold equity in Sofie Biosciences and Trethera Therapeutics. Intellectual property has been patented by the University of California and has been licensed to Sofie Biosciences and Trethera Therapeutics. This intellectual property was not used in the current study. No other potential conflict of interest relevant to this article was reported.

Keywords

PSMA expression; prostate cancer; radioligand therapy; ^{177}Lu -PSMA; ^{225}Ac -PSMA617; resistance

INTRODUCTION

The prostate specific membrane antigen (PSMA) is a plasma membrane glycoprotein highly over-expressed in metastatic castration-resistant (mCR) prostate cancer (PC). It has been associated with cell migration, invasiveness, folate uptake, bone metastases, and poor prognosis (1). PSMA-targeting radioligands bind with high affinity to the extracellular domain of PSMA and deliver ionizing radiation predominantly to PSMA-positive cells. Radioligand therapy (RLT) with ^{177}Lu -PSMA (and ^{225}Ac -PSMA) has been introduced as a late-stage therapeutic alternative in mCRPC. Data from clinical studies suggest that PSMA-RLT is effective in patients with mCRPC as it delays disease progression, reduces serum prostate specific antigen levels, and improves bone pain (2–4).

Eligibility for PSMA-RLT depends, among others, on PSMA expression on ^{68}Ga -PSMA positron emission tomography/computed tomography (PET/CT) images. More than 90% of mCRPC patients present with PSMA-positive lesions (5). However, ~50% of mCRPC patients do not respond to PSMA-RLT despite documented PSMA expression (2,4). Potential resistance mechanisms include insufficient tumor radiation dose, upregulated DNA damage response pathways, germline or somatic mutations, and low or heterogeneous tumor PSMA expression. The degree of PSMA expression likely affects tumor cell ^{177}Lu -/ ^{225}Ac -PSMA uptake. ^{177}Lu / ^{225}Ac cytotoxicity is a consequence of DNA single and double strand breaks induced by beta particles (6,7). Therefore, the degree of PSMA-radioligand uptake is likely associated with the degree of DNA damage and tumor cell death.

Here we investigated PSMA-RLT efficacy as a function of tumor PSMA expression levels. We also modeled tumor heterogeneity by creating subcutaneous (s.c.) xenografts with various fractions of PSMA-positive tumor cells to assess RLT responses. We aimed to determine whether a threshold value for minimum PSMA levels required for therapeutic response exists.

MATERIALS AND METHODS

Study design

Study 1: ^{177}Lu -PSMA617 RLT efficacy as function of PSMA expression/cell (Figure 1A). RM1-YFP (PSMA-, YFP-only), RM1-PSMA low (PSMA⁺; $\sim 0.5 \times 10^4$ PSMA/cell), RM1-PSMA medium (PSMA⁺⁺; $\sim 1.3 \times 10^4$ PSMA/cell), and RM1-PSMA high (PSMA⁺⁺⁺; $\sim 4.9 \times 10^4$ PSMA/cell; Supplementary Figure S1A), respectively, were injected into Nod Scid gamma (NSG) mice (12 mice/group; day 0) to generate xenografts.

Study 2: The impact of the fraction of PSMA-positive vs. PSMA-negative RM1 tumor cells on ^{177}Lu -PSMA617 RLT efficacy (Figure 2A). PSMA- and PSMA⁺⁺⁺ cells were

mixed at different ratios (PSMA⁻: PSMA⁺⁺⁺ = 100:0, 75:25, 50:50, 25:75, 0:100) and injected into NSG mice (10 mice/group; day 0).

Study 3: To confirm the data obtained in the RM1 model, we tested the relevance of PSMA expression for RLT outcome in a human-derived PC model (study 3; Figure 3A). NSG mice were injected with PC-3-PIP (PSMA⁺⁺⁺) and PC-3 (PSMA⁻) at different ratios (PSMA⁻: PSMA⁺⁺⁺ = 100:0, 66:33, 66:33, 0:100; 12 mice/group). The ratios of PSMA-positive to -negative cells was changed to 0-33-66-100% based on the results of study 2 (Figure 2B, Supplementary Figure S4A).

Study 4: Lastly, to further elucidate the consequences of PSMA heterogeneity, PSMA⁻ and PSMA⁺⁺⁺ RM1 cells were mixed at different ratios (PSMA⁻: PSMA⁺⁺⁺ = 100:0, 66:33, 66:33, 0:100) and injected into NSG mice (10 mice/group; day 0) for treatment with ²²⁵Ac-PSMA617 (Figure 4A).

Baseline tumor volume was determined on day 4 (RM1 model) or day 19 (PC-3 model). One to two days later, mice were treated with ¹⁷⁷Lu-PSMA617 (studies 1, 2, 3), or ²²⁵Ac-PSMA617 (study 4). Tumor volume was measured 3x/week (RM1 model) or 1–2x/week (PC-3 model) by CT volumetry. In the RM1 model, tumor growth studies were terminated already at day 14 post RLT because of tumor size and mouse condition (beginning ulceration) as per veterinarian instruction. Absolute tumor volumes for all studies are shown in Supplementary Figure S2A–D.

In a subset of mice (3 mice/group; randomized group allocation), tumors were resected 2 days post RLT. We chose this time point based on our preliminary biodistribution data (data not shown) which suggested a higher ¹⁷⁷Lu-PSMA617 uptake at 48h vs. 4h following injection of 30 MBq ¹⁷⁷Lu-PSMA617 into mice with C4–2 tumors. The percent injected ¹⁷⁷Lu-/²²⁵Ac-PSMA617 activity incorporated into the tumors was determined by *ex vivo* gamma-counting. DNA damage and PSMA expression in the tumor samples were analyzed by anti-53BP1 and anti-PSMA immunohistochemistry (IHC), respectively.

To ensure comparable tumor growth characteristics across groups and for comparison to tumor volumes in RLT-treated mice tumor volumes of untreated mice were measured by CT (5 mice/group).

Cell culture

Murine RM1 (ATCC CRL-3310) sublines expressing no, low, medium, or high levels of human PSMA were described previously (8,9). PC-3 were provided by K. Pillarsetty (Memorial Sloan Kettering Cancer Center, USA). C4–2 were a kind gift from G. Thalmann (University of Bern, Switzerland). 22Rv1 cells were purchased from ATCC (CRL-2505). Cells were thawed 2–3 weeks prior to injection into mice. Cells were maintained in Rosewell Park Memorial Institute (RPMI)-1640 medium supplemented with 10% fetal bovine serum (Omega Scientific) at 37°C, 5% CO₂ and 20% O₂. Contamination with mycoplasma was excluded before preparing the cells for injection into mice using the Venor™ GeM Mycoplasma Detection Kit (Sigma-Aldrich). Human cell lines were

authenticated in August or September 2019 using the Promega powerplex16 System and the small tandem repeat alleles were searched on the DSMZ database (Laragen, Inc.).

Mice

All studies were approved by the UCLA Animal Research Committee (#2005–090). Intact male, 6–8 weeks old NSG mice were obtained from the UCLA Radiation Oncology Animal Core. Mice housed under pathogen-free conditions with food and water ad libitum, and a 12–12 hour light-dark cycle. Veterinarian staff and investigators observed the mice daily to ensure animal welfare and determine if humane endpoints (e.g., hunched and ruffled appearance, apathy, ulceration, severe weight loss, tumor burden) were reached. All interventions were performed under anesthesia (2% isoflurane). RM1 (a total of 0.1×10^6 cells in PBS: Matrigel = 1:1) or PC-3 sublines (a total of 5×10^6 cells in 100 μ l Matrigel) were inoculated s.c. into the left shoulder region. Mice weighed (mean \pm SD) 30.9 \pm 2.8 g (study 1), 29.5 \pm 2.0 g (study 2), 28.7 \pm 1.3 g (study 3), and 25.5 \pm 0.6 g (study 4) at study start, and 29.2 \pm 3.2 g (study 1), 31.4 \pm 2.7 g (study 2), 25.6 \pm 3.4 g (study 3), and 29.6 \pm 0.75 g (study 4) at the endpoint.

CT volumetry

Tumor volume was analyzed by CT as previously described (8–10). Briefly, using OsiriX v.10.0.2 (Pixmeo SARL), tumors were delineated on 7 CT slices and the compute volume function was used to derive the tumor volume.

^{177}Lu -PSMA617 RLT

In studies 1 and 2 (RM1 model), mice received 60 MBq of ^{177}Lu -PSMA617 (84 GBq/ μ mol; UCLA Biomedical Cyclotron Facility) intravenously into the tail vein (9). In study 3 (PC-3 model), mice received 40 MBq ^{177}Lu -PSMA617 (84 GBq/ μ mol) (11).

^{225}Ac -PSMA617 therapy

In study 4, mice with RM1 tumors received 40 kBq ^{225}Ac -PSMA617 (130 MBq/ μ mol; UCLA Biomedical Cyclotron Facility) intravenously into the tail vein. For synthesis, [^{225}Ac]Ac(NO₃)₃ was acquired through the Isotope Program, Office of Nuclear Physics, Department of Energy's Office of Science, and dissolved in 0.1 M HCl. Labeling of the precursor PSMA617 (in 1 M NaOAc/10 mg/mL gentisic acid) with the ^{225}Ac -solution commenced at 90°C, 30 min, pH ~5.5, and resulted in ^{225}Ac -PSMA617 (>92% purity by radio thin-layer chromatography).

Tumor biodistribution

For ^{177}Lu -treated tumors, tumors were resected, weighed and incorporated activity was measured in a gamma-counter (Cobra II Auto-Gamma; Packard Instrument Co.) with ^{177}Lu detection energy window of 189 – 231 keV. Gamma counting was delayed 24h for the ^{225}Ac -treated tumors to allow ^{225}Ac to reach the secular equilibrium state with its daughter nuclides. The activity of ^{225}Ac was inferred from ^{221}Fr counts detected in the energy window with limits 170–260 keV. Data were decay corrected to the time of tumor resection and expressed as percent injected activity per gram tissue (%IA/g).

Immunohistochemistry

Tumor tissues were stained for the DNA damage marker 53BP1 and PSMA as previously described (9). Briefly, tissues were fixed in 10% formalin overnight and transferred to 70% ethanol for storage until radioactivity had decayed. Paraffin-embedded sections (4 μ m) were de-paraffinized and re-hydrated. Endogenous peroxidase was blocked (3% hydrogen peroxide/methanol, 10 min.). Antigens were retrieved in heated 0.01 M citrate buffer, pH 6.0 (95°C, 25 min.). Specimens were incubated overnight at 4°C with a polyclonal rabbit anti 53BP1 antibody (1:2000; Novus, NB100–304) or a mouse anti-PSMA antibody (clone 3E6; 1:50, DAKO, M362029–2) in bovine serum albumin. For detection, the Dakocytomation Envision System labeled polymer horseradish peroxidase (DakoCytomation, Carpinteria) and the diaminobenzidine reaction (#BDB2004 L; Biocare Medical) were used according to the manufacturers' instructions. The sections were counterstained with hematoxylin. All slides were mounted with Cytoseal (Fisher Scientific) and scanned digitally at 20x magnification using ScanScope AT (Leica Biosystems, Vista).

For xenografts, semiautomated analysis of samples was performed using the Definiens Developer XD and Tissue Studio (Definiens AG). The immunoreactive score (IRS) was calculated by multiplying the staining intensity with the percent positive cells in the sample. For comparison of the relative PSMA expression between experimental groups in studies 2–4, a relative IRS was calculated by correcting for background staining (IRS of interest – IRS of PSMA- tumors) and normalization to the 100% PSMA⁺⁺⁺ group (i.e., 100% group = 100%).

PSMA expression on human samples was determined using a tissue microarray. This array (kind gift of Dr. J. Said, UCLA) contained human prostatectomy samples from 76 patients. For each patient, matched normal and tumor tissue specimen (3 each) were available. A total of 199 tumor samples were available for analysis (29 samples without core or diagnostic material in the core). Analysis was performed by an experienced pathologist (DD) using a semi-quantitative scoring system (0 = negative, 1 = weak, 2 = strong staining).

Flow cytometry

Cells (0.2–0.5 \times 10⁶) were stained with an anti-hPSMA-APC antibody (dilution 1:10, incubation for 30 min. at 4°C in the dark; clone REA408, Miltenyi Biotec). Absolute PSMA antigenic sites on RM1 and C4–2 lines were determined using the QuantumTM Simply Cellular[®] human IgG beads (Bang Laboratories) according to the manufacturer's instructions. Samples were measured on a 5-laser LSR II cytometer (BD) and analyzed using FlowJo (Three Star) software.

In vitro radiosensitivity

RM1 sublines were seeded on 6-well plates (5,000 cells/well). On the next day, cells were irradiated (x-ray) with 2 Gy or 5 Gy (dose rate 5.4 Gy/min; x-ray energy 300 kV at 10 mA, filtration 1.5 mm Cu and 3 mm Al resulting in a half value layer of 3.0 mm Cu) or left untreated. Days to reach confluence were recorded as a measure of radiosensitivity. Alternatively, on day 4 (RM1) or day 6 (PC-3) after seeding, cells were pre-fixed by adding 4% formaldehyde/PBS to the culture medium for 2–5 min. before medium removal and

fixation with 4% formaldehyde/PBS for 15 min. Cells were stained with crystal violet solution (0.05% w/v crystal violet/MilliQ-water; 15 min.), washed (3–4 times, water) and dried.

***In vitro* ¹⁷⁷Lu-PSMA617 binding assay**

RM1 cells (10^5 cells/well) were seeded in triplicates for each condition and incubated overnight. Cells were washed once with RPMI-1640/5% bovine serum albumin (binding medium) and incubated for 30 min. in binding medium before addition of ¹⁷⁷Lu-PSMA617 (0.2 nM = 4.2 kBq per well). To determine specific binding, the PSMA inhibitor 2-(Phosphonomethyl)pentane-1,5-dioic acid (PMPA; 10 μ M) was added to one triplicate per cell line. Following 1h incubation at 37°C, supernatant was transferred to gamma-counting tubes. Cells were washed with glycine.HCl pH 2.8 to remove membrane-bound radioligand and the wash solution was collected into a second set of tubes. Using 0.3N NaOH, cells were lysed and collected into a third set of tubes. All samples were measured in a gamma-counter (see above). Data were decay corrected to the time of radiosynthesis completion. For analysis, the percent activity in the supernatant, membrane-bound, internalized, and overall taken up were determined. Specific binding was calculated by subtracting the values from samples incubated with PMPA from those of samples without inhibitor. Data were normalized to the cell number which was determined in triplicate on the day of the experiment for each cell line.

Statistical analysis

Data are presented as mean \pm standard deviation (SD). One-way ANOVA with Holm-Sidak correction for multiple testing was used to compare multiple groups. Significance was set at $p < 0.05$. Non-linear centered second order polynomial regression was used for regression analyses unless indicated otherwise. GraphPad Prism (version 7, GraphPad Software, Inc.) was used for all statistical analyses. Data were analyzed blinded. A power analysis was performed (G*Power3.1) in relation to the primary goal of comparing tumor growth between experimental groups using the following parameters: t-test for difference in mean of independent groups, alpha error 0.05, effect sizes of 1.3 SD (9,10), 80% power.

RESULTS

Human PC presents with heterogenous PSMA expression

To corroborate our hypothesis that heterogenous PSMA expression could attenuate PSMA-RLT efficacy in PC patients, we analyzed PSMA positivity in PC specimens. Per semi-quantitative analysis of PSMA expression, 48/199 (24%) samples scored 0, 26/199 (13%) scored 1+, 67/199 (34%) scored 2+, and 58/199 (29%) scored 3+. In line with previous studies (12–15), we thus confirmed PSMA heterogeneity on a per cell (varying PSMA staining intensity) and per lesion (spatial differences) basis (Supplementary Figure S3).

PSMA expression intensity per cell translates into RLT efficacy

To determine ¹⁷⁷Lu-PSMA617 efficacy as function of cellular PSMA expression levels (Figure 1A, study 1) we used RM1 sublines with varying levels of PSMA (PSMA-, PSMA⁺, PSMA⁺⁺, PSMA⁺⁺⁺) (Supplementary Figures S1A). Differences in PSMA expression were

maintained *in vivo* and did not affect general radiosensitivity (x-ray) of these cells *in vitro* or tumor growth *in vivo* (Supplementary Figure S1B–E).

PSMA-RLT induced the most pronounced growth retardation in PSMA⁺⁺⁺, followed by PSMA⁺⁺ (PSMA⁺⁺ vs. PSMA⁺⁺⁺, $p=0.0015$) and PSMA⁺ tumors (PSMA⁺ vs. PSMA⁺⁺, $p=0.0016$). The low PSMA expression on PSMA⁺ was sufficient for an anti-tumor effect of RLT (PSMA⁺ vs. PSMA⁻, $p<0.0001$). Tumors without PSMA expression did not respond to RLT ($p<0.0001$ PSMA⁻ vs. PSMA⁺; PSMA⁻ RLT vs. untreated, $p=0.3517$) (Figure 1B; Supplementary Table S1 and Figure S1C).

PSMA expression level correlates with ¹⁷⁷Lu-PSMA617 tumor uptake

To investigate if the differences in PSMA-RLT efficacy across groups could be explained by differential ¹⁷⁷Lu-PSMA617 uptake, we measured ¹⁷⁷Lu-PSMA617 activity *in vitro* and in resected tumors. In line with published data (16), ¹⁷⁷Lu-PSMA617 effectively bound to cells in a PSMA-dependent manner and a large fraction of the activity was internalized. We confirmed a near perfect correlation between radioligand binding and PSMA expression (flow cytometry vs. membrane-bound activity, $R^2=0.9490$; vs. internalized activity, $R^2=0.9992$; vs. overall uptake, $R^2=0.9992$; Supplementary Figure S1F).

Similarly, and in agreement with the tumor growth data, ¹⁷⁷Lu-PSMA617 tumor uptake positively correlated with *in vitro* ¹⁷⁷Lu-PSMA617 binding ($R^2=0.9924$; Supplementary Figure S1F) and cell surface PSMA expression ($R^2=0.9797$; PSMA⁺⁺⁺ vs. PSMA⁺⁺, $p<0.0001$; PSMA⁺⁺ vs. PSMA⁺, $p=0.0959$; PSMA⁺ vs. PSMA⁻, $p=0.7789$) (Figure 1C–D, Supplementary Table S1 and Figure S1D).

¹⁷⁷Lu-PSMA617 uptake correlates with DNA damage

To further explore the mechanistic basis for the PSMA dependent differences in therapeutic efficacy, we quantified DNA damage in the resected tumors. The number of 53BP1 foci tended to increase with ¹⁷⁷Lu-PSMA617 uptake ($R^2=0.9803$) (Figure 1G) and with higher tumor cell PSMA levels ($R^2=0.7154$; PSMA⁺⁺⁺ vs. PSMA⁺⁺, $p=0.1473$; PSMA⁺⁺ vs. PSMA⁺, $p=0.3563$; PSMA⁺ vs. PSMA⁻, $p=0.6483$) (Figure 1E, F, H; Supplementary Table S1).

Higher proportion of PSMA-positive tumor cells improves targeting with ¹⁷⁷Lu-PSMA617

Next, we tested the efficacy of PSMA-RLT as function of PSMA-positive to -negative cell ratios in a given tumor (Figure 2A, study 2). Following injection of 0, 25, 50, 75, and 100% PSMA-positive RM1 tumor cells, respectively, we cross-checked PSMA expression in the resulting xenografts (Supplementary Figure S4). The presence of stroma/connective tissue resulted in <100% cancer cells in all cases. However, comparison of PSMA IRS in between experimental groups was in line with the percent PSMA-positive cells injected, except for the group 25% PSMA-positive tumor cells. Relative PSMA IRS were (mean±SD): group “100%”, $100\pm 13.9\%$; group “75%”, $75.5\pm 18.2\%$; group “50%”, $54.2\pm 6.2\%$; group “25%”, $50.2\pm 5.7\%$; group “0%”, $0\pm 0\%$.

Tumors containing only PSMA⁺⁺⁺ or PSMA⁻ tumor cells, respectively, exhibited similar responses to ¹⁷⁷Lu-PSMA617 as in study 1. Effectiveness of ¹⁷⁷Lu-PSMA617 increased with increasing fractions of PSMA-positive tumor cells (100 vs. 75%, p=0.0177; 75 vs. 50%, p=0.0012; 50 vs. 25%, p=0.5492; 25 vs. 0%, p<0.0001). Congruent with the presence of ~50% PSMA-positive tumor cells in the 25% groups, the difference in tumor growth between the groups 25% and 50% PSMA⁺⁺⁺ cells was not significant (Figure 2B; Supplementary Table S1).

Association between ¹⁷⁷Lu-PSMA617 uptake and DNA damage in tumors with heterogeneous PSMA expression

¹⁷⁷Lu-PSMA617 uptake in resected tumors 2 days post-RLT tended to increase proportionally with the fraction of PSMA-positive cells ($R^2=0.9398$; 100 vs. 75%, p=0.7318; 75 vs. 50%, p=0.4701; 50 vs. 25%, p=0.7318; 25 vs. 0%, p=0.0042) (Figure 2C; Supplementary Table S1 and Figure S4B).

Similarly, the number of 53BP1 foci tended to be higher in experimental groups with a higher fraction of PSMA-positive cells ($R^2=0.9372$; 100 vs. 75%, p=0.3330; 75 vs. 50%, p=0.9036; 50 vs. 25%, p=0.9787; 25 vs. 0%, p=0.9036) and higher ¹⁷⁷Lu-PSMA617 uptake ($R^2=0.9861$) (Figure 2D–F; Supplementary Table S1).

Relevance of intra-lesion PSMA heterogeneity for ¹⁷⁷Lu-PSMA617 efficacy in a human-derived PC model

To confirm our findings obtained in RM1 tumors in a human PC derived model we investigated the impact of PSMA heterogeneity in PC-3 based xenografts (Figure 3A). PC-3 cells grow slower *in vivo* than RM1 cells (Supplementary Figure S2), and express ~11x more PSMA than PSMA⁺⁺⁺ RM1 cells (Supplementary Figure S1A). PC-3 (PSMA⁻) and PC-3-PIP (PSMA⁺⁺⁺) displayed similar radiosensitivity (x-ray) *in vitro* and tumor growth *in vivo* (Supplementary Figure S5).

Following injection of PC-3: PC-3-PIP cells in ratios of 0:100, 33:66, 66:33, or 100:0, relative PSMA IRS in tumors were (mean±SD): group “100%”, 100.0±36.3%; group “66%”, 41.3±11.7%; group “33%”, 19.2±7.9 %; and group “0%”, 0.0±0.0%. Treatment with ¹⁷⁷Lu-PSMA617 resulted in tumor shrinkage and effective disease control in mice with PC-3-PIP but not with PC-3 tumors. As in the RM1 model, the fraction of (PSMA-positive) PC-3-PIP cells was correlated with ¹⁷⁷Lu-PSMA617 RLT efficacy (100 vs. 66%, p<0.0001; 66 vs. 33%, p=0.0001; 33 vs. 0%, p<0.0001; 0% vs. untreated PSMA⁻ tumors, p=0.9787) (Figure 3B; Supplementary Table S1 and Figure S5D); at the end of the observation period (day 88), 9/9 mice were alive in the group “100%” PSMA-positive cells, 5/9 in “66%”, and 0/9 mice in the groups “0%” and “33%” PSMA-positive cells, respectively.

Consistently, ¹⁷⁷Lu-PSMA617 uptake ($R^2=0.9827$) and DNA damage ($R^2=0.7910$) were correlated with PSMA expression in the PC-3 model (uptake: 100 vs. 66%, p<0.0001; 66 vs. 33%, p=0.0046; 33 vs. 0%, p=0.0009; 53BP1: 100 vs. 66%, p=0.0159; 66 vs. 33%, p=0.05838; 33 vs. 0%, p=0.4323) (Figure 3C–F; Supplementary Table S1 and Figure S5E, F).

Taken together, studies 1–3 suggest that degree of PSMA expression is correlated with ^{177}Lu -PSMA617 uptake and degree of DNA damage, all resulting in a better therapeutic outcome.

Efficacy of ^{225}Ac -PSMA in tumors with heterogeneous PSMA expression

PSMA heterogeneity may increase the reliance on the crossfire effect for effective tumor targeting (study 4; Figure 4A). To test this hypothesis, we treated mice with tumors containing various fractions of PSMA-positive tumor cells with ^{225}Ac -PSMA617 which has a shorter range in tissue than ^{177}Lu .

In agreement with injection of 0, 33, 66, or 100% PSMA⁺⁺⁺ RM1 cells, relative PSMA IRS in resected tumors were (mean \pm SD): group “100%”, 100 \pm 34.4%; group “66%”, 62 \pm 3.6%; group “33%”, 34 \pm 7.7 %; group “0%”, 0 \pm 0%.

Similar to ^{177}Lu -PSMA617, effectiveness of ^{225}Ac -PSMA617 increased with increasing fractions of PSMA-positive tumor cells (100% vs. 66%, $p=0.0020$; 66% vs. 33%, $p=0.0028$; 33% vs. 0%, $p=0.0120$; 0% vs. untreated PSMA- tumors, $p=0.5401$). Differences between groups tended to be more accentuated (studies 2 vs. 4). Overall, treatment with ^{225}Ac -PSMA617 resulted in improved tumor control, higher tracer uptake and DNA damage levels compared to ^{177}Lu -PSMA617 RLT (Figure 4B; Supplementary Table S1 and Figure S6).

In agreement with the differences in therapeutic efficacy between groups, ^{225}Ac -PSMA617 uptake correlated with the fraction of PSMA-positive cells in resected tumors ($R^2=0.9967$; 100 vs. 66%, $p=0.0291$; 66 vs. 33%, $p=0.0532$; 33 vs. 0%, $p=0.0416$). Correspondingly, higher uptake resulted in enhanced DNA damage ($R^2=0.8329$; 100 vs. 66%, $p=0.0497$; 66 vs. 33%, $p=0.3142$; 33 vs. 0%, $p=0.3142$) (Figure 4C–F; Supplementary Table S1 and Figure S6).

Thus, while radioisotopes with long ranges in tissue may, at least partly, be able to compensate for PSMA heterogeneity because of their crossfire, the higher linear energy transfer of isotopes like ^{225}Ac may still result in enhanced radiation-induced cytotoxicity.

DISCUSSION

Here we investigated whether PSMA expression/cell and the fraction of PSMA-positive cells, as markers of tumor heterogeneity, are determinants of RLT efficacy in murine models of prostate cancer. We demonstrate that both are critically important for effective tumor targeting with PSMA-RLT: The PSMA expression level is proportional to the radioligand tumor uptake which, in turn, is associated with the degree of DNA damage.

Several studies have demonstrated intra-patient variations in both PSMA expression and the fraction of PSMA-positive cells in given tumors. These variations can arise (i) from dynamic processes (12–14,17–19), including drug-induced alterations (10,20–23); (ii) from the presence of highly PSMA expressing neovasculature in cancer types without PSMA expression in tumor cells (5,14,17,24–27); and (iii) from areas within the tumor containing PSMA-negative cells (12,13). PSMA heterogeneity might still result in positive image

contrast on ^{68}Ga -PSMA PET scans (24,28–30) and thus, in the decision to administer RLT. Therefore, PSMA heterogeneity might be an underappreciated contributor to RLT failure.

Currently, differences in PSMA expression can most accurately be captured by analyzing tumor biopsies (e.g., IHC). However, biopsying every lesion is not feasible in mCRPC patients. A potential future alternative to biopsies may be the radiomic analysis of ^{68}Ga -PSMA tumor uptake in which phenotypic information is extracted from PET/CT images (31–33). Because of the limitations of radiomics (34,35) and biopsies, clinicians rely on “expression levels” by means of PET standardized uptake values (SUV) and ^{68}Ga -PSMA uptake above liver activity in the majority of metastases (but not necessarily in all) is considered a condition for RLT initiation (4,37). SUVs inform about inter-lesion PSMA heterogeneity but can be confounded by small lesion size (partial-volume effect). PET imaging cannot, or only to a limited extent (36), resolve intra-lesion heterogeneity although intra-lesion heterogeneity/homogeneity in target expression might be one factor underlying inter-lesion differences in ^{68}Ga -PSMA SUVs.

The present study suggests that low PSMA expression is associated with markedly attenuated, yet still measurable RLT effects. This finding is in line with the observation that the overall lower PSMA expression in PSMA-negative tumors with PSMA-positive neovasculature was sufficient for an anti-tumor-effect of ^{111}In -J591, a radio-labelled PSMA-binding antibody (26). However, undertreatment not only reduces RLT efficacy, but might also select treatment resistant tumor clones.

One solution to account for potential intra- and inter-lesion PSMA heterogeneity and to optimize safely delivered maximal tumor doses is individual patient dosimetry (38–41). This approach provides overall tumor radiation dose measurements independent of intra- and inter-lesional PSMA heterogeneity. Presently, patients usually receive a standard activity (mostly ~7 GBq) without dosimetric considerations of the maximal doses that could be achieved with minimal healthy organ damage. However, using dosimetry and pharmacodynamic modeling, it has been suggested that lesions with high PSMA expression could be treated with activities higher than the standard activity without exceeding the tolerable biological effective dose for organs at risk such as kidney and salivary glands (42–44). Therefore, it seems feasible to optimize RLT efficacy in patients with high and homogenous PSMA expression by increasing the administered activity (and peptide amount). In patients with low PSMA levels and/or high inter-lesion heterogeneity, dosimetry might help to determine whether the tumor absorbed doses that could be achieved are sufficient to induce a significant therapeutic effect. It would also indicate the fraction of metastases that could be targeted successfully vs. the number of metastases that would likely receive an insufficient dose. Therefore, dosimetry would provide valuable information for the decision whether to initiate RLT or to choose an alternative treatment regimen. By treating only those patients who are likely to benefit, more patients would be spared an unsuccessful (and costly) treatment regimen, and success rates of RLT would be increased.

It is possible that PSMA-PET/CT uptake intensity as measured by SUV parameters may be predictive of response/non-response to RLT (e.g., definition of a SUV cut-off). Uptake intensity by PET may correlate with absorbed doses which in turn may contribute to

optimizing RLT activities (45,46). Indeed, first clinical data suggest that ^{68}Ga -PSMA uptake (SUV) on pre-therapy PET/CT correlates with the absorbed ^{177}Lu -PSMA dose and prostate specific antigen response (37,47,48). Consistently, a recent ^{177}Lu -PSMA RLT clinical trial in which patients with low ^{68}Ga -PSMA relative to ^{18}F -fluorodeoxyglucose uptake were excluded (4) reported higher response rates than reported for less stringently selected patients (2). A potential limitation of both, dosimetry- and PSMA-PET/CT-based approaches is the presence of PSMA negative lesions that might remain undetected and can give rise to tumor relapse. Thus, patients may benefit from additional PET/CT scans with an alternative tracer (e.g., fluorodeoxyglucose) (4). A further cause for relapse not captured by dosimetry or PET might be micrometastatic disease below the imaging detection limit.

RLT efficacy might be improved by pharmacological upregulation of PSMA (21). In the present study, increases in target availability positively correlated with ^{177}Lu - ^{225}Ac -PSMA617 tumor uptake and anti-tumor effect. This finding is in line with a study showing higher uptake of a PSMA-binding PET probe in LNCaP vs. 22Rv1 (lower PSMA expression than LNCaP) xenografts (49). The RM1 models used here express similar PSMA levels as 22Rv1, but at least 5x and 11x less PSMA than C4-2 and PC-3-PIP, respectively (Supplementary Figure S1A). We previously showed that drug-induced PSMA upregulation in C4-2 tumors did not enhance ^{177}Lu -PSMA617 efficacy (10). Therefore, while patients with low PSMA uptake on PET/CT might benefit from PSMA induction, increases in PSMA levels beyond a certain, yet to be defined threshold, might not improve RLT outcome.

Lastly, low-dose irradiation (x-ray) of tumors was shown to enhance cancer immunotherapy by re-programming macrophages to a state that promotes tumor infiltration and cell kill by cytotoxic T cells (50). It is thus possible that - in immunocompetent animal models and in patients - RLT against low PSMA expression tumors may synergize with immunotherapy.

CONCLUSION

PSMA RLT is effective even in tumors with low PSMA levels or with a small number of PSMA-positive cells. However, optimal anti-tumor efficacy of RLT hinges, among other factors, on homogeneously high target expression. Clinical studies designed to determine intra- and inter-lesion PSMA heterogeneity and to optimize PSMA-RLT for each patient are highly warranted.

Supplementary Material

Refer to Web version on PubMed Central for supplementary material.

ACKNOWLEDGEMENTS

We thank Liu Wei for assistance with radioligand injections and acknowledge the UCLA Translational Pathology Core Laboratory and Rana Riahi for IHC stainings.

Financial support. This study was partially funded by the US Department of Energy, Office of Science Award (DE-SC0012353), the Prostate Cancer Foundation (17CHAL02) and the UCLA SPORE in Prostate Cancer (P50 CA092131). KL received a scholarship from the German Research Foundation (Deutsche Forschungsgemeinschaft, DFG, grant 807454).

REFERENCES

1. O'Keefe DS, Bacich DJ, Huang SS, Heston WDW. A Perspective on the Evolving Story of PSMA Biology, PSMA-Based Imaging, and Endoradiotherapeutic Strategies. *J Nucl Med* 2018;59:1007–13 [PubMed: 29674422]
2. Rahbar K, Ahmadzadehfard H, Kratochwil C, Haberkorn U, Schäfers M, Essler M, et al. German Multicenter Study Investigating ¹⁷⁷Lu-PSMA-617 Radioligand Therapy in Advanced Prostate Cancer Patients. *J Nucl Med* 2017;58:85–90 [PubMed: 27765862]
3. Fendler WP, Rahbar K, Herrmann K, Kratochwil C, Eiber M. (177)Lu-PSMA Radioligand Therapy for Prostate Cancer. *J Nucl Med* 2017;58:1196–200 [PubMed: 28663195]
4. Hofman MS, Violet J, Hicks RJ, Ferdinandus J, Thang SP, Akhurst T, et al. ¹⁷⁷Lu-PSMA-617 radionuclide treatment in patients with metastatic castration-resistant prostate cancer (LuPSMA trial): a single-centre, single-arm, phase 2 study. *Lancet Oncol* 2018;19:825–33 [PubMed: 29752180]
5. Silver DA, Pellicer I, Fair WR, Heston WD, Cordon-Cardo C. Prostate-specific membrane antigen expression in normal and malignant human tissues. *Clin Cancer Res* 1997;3:81–5 [PubMed: 9815541]
6. Nonnekens J, van Kranenburg M, Beerens CE, Suker M, Doukas M, van Eijck CH, et al. Potentiation of Peptide Receptor Radionuclide Therapy by the PARP Inhibitor Olaparib. *Theranostics* 2016;6:1821–32 [PubMed: 27570553]
7. Graf F, Fahrer J, Maus S, Morgenstern A, Bruchertseifer F, Venkatachalam S, et al. DNA double strand breaks as predictor of efficacy of the alpha-particle emitter Ac-225 and the electron emitter Lu-177 for somatostatin receptor targeted radiotherapy. *PLoS One* 2014;9:e88239 [PubMed: 24516620]
8. Lückerrath K, Stuparu AD, Wei L, Kim W, Radu CG, Mona CE, et al. Detection Threshold and Reproducibility of ⁶⁸Ga-PSMA11 PET/CT in a mouse model of prostate cancer. *J Nucl Med* 2018;59:1392–7 [PubMed: 29602819]
9. Fendler WP, Stuparu AD, Evans-Axelsson S, Luckerath K, Wei L, Kim W, et al. Establishing (177)Lu-PSMA-617 Radioligand Therapy in a Syngeneic Model of Murine Prostate Cancer. *J Nucl Med* 2017;58:1786–92 [PubMed: 28546332]
10. Lückerrath K, Wei L, Fendler WP, Evans-Axelsson S, Stuparu AD, Slavik R, et al. Preclinical evaluation of PSMA expression in response to androgen receptor blockade for theranostics in prostate cancer. *EJNMMI Res* 2018;8:96 [PubMed: 30374743]
11. Wang Z, Tian R, Niu G, Ma Y, Lang L, Szajek LP, et al. Single Low-Dose Injection of Evans Blue Modified PSMA-617 Radioligand Therapy Eliminates Prostate-Specific Membrane Antigen Positive Tumors. *Bioconjug Chem* 2018;29:3213–21 [PubMed: 30105912]
12. Hupe MC, Philippi C, Roth D, Kümpers C, Ribbat-Idel J, Becker F, et al. Expression of Prostate-Specific Membrane Antigen (PSMA) on Biopsies Is an Independent Risk Stratifier of Prostate Cancer Patients at Time of Initial Diagnosis. *Front Oncol* 2018;8:623 [PubMed: 30619757]
13. Mannweiler S, Amersdorfer P, Trajanoski S, Terrett JA, King D, Mehes G. Heterogeneity of prostate-specific membrane antigen (PSMA) expression in prostate carcinoma with distant metastasis. *Pathol Oncol Res* 2009;15:167–72 [PubMed: 18802790]
14. Gorges TM, Riethdorf S, von Ahnen O, Nastal YP, Röck K, Boede M, et al. Heterogeneous PSMA expression on circulating tumor cells: a potential basis for stratification and monitoring of PSMA-directed therapies in prostate cancer. *Oncotarget* 2016;7:34930–41 [PubMed: 27145459]
15. Paschalis A, Sheehan B, Riisnaes R, Rodrigues DN, Gurel B, Bertan C, et al. Prostate-specific Membrane Antigen Heterogeneity and DNA Repair Defects in Prostate Cancer. *Eur Urol* 2019
16. Benešová M, Schäfer M, Bauder-Wüst U, Afshar-Oromieh A, Kratochwil C, Mier W, et al. Preclinical Evaluation of a Tailor-Made DOTA-Conjugated PSMA Inhibitor with Optimized Linker Moiety for Imaging and Endoradiotherapy of Prostate Cancer. *J Nucl Med* 2015;56:914–20 [PubMed: 25883127]
17. Ben Jemaa A, Bouraoui Y, Sallami S, Banasr A, Noura Y, Horchani A, et al. Cellular distribution and heterogeneity of Psa and Psma expression in normal, hyperplasia and human prostate cancer. *Tunis Med* 2013;91:458–63 [PubMed: 24008878]

18. Bronsert P, Reichel K, Ruf J. Loss of PSMA Expression in Non-neuroendocrine Dedifferentiated Acinar Prostate Cancer. *Clin Nucl Med* 2018;43:526–8 [PubMed: 29659395]
19. Ren H, Zhang H, Wang X, Liu J, Yuan Z, Hao J. Prostate-specific membrane antigen as a marker of pancreatic cancer cells. *Med Oncol* 2014;31:857 [PubMed: 24477651]
20. Kranzbühler B, Salemi S, Umbricht CA, Müller C, Burger IA, Sulser T, et al. Pharmacological upregulation of prostate-specific membrane antigen (PSMA) expression in prostate cancer cells. *Prostate* 2018;78:758–65 [PubMed: 29633296]
21. Murga JD, Moorji SM, Han AQ, Magargal WW, DiPippo VA, Olson WC. Synergistic co-targeting of prostate-specific membrane antigen and androgen receptor in prostate cancer. *Prostate* 2015;75:242–54 [PubMed: 25327687]
22. Hope TA, Truillet C, Ehman EC, Afshar-Oromieh A, Aggarwal R, Ryan CJ, et al. 68Ga-PSMA-11 PET Imaging of Response to Androgen Receptor Inhibition: First Human Experience. *J Nucl Med* 2017;58:81–4 [PubMed: 27660139]
23. Meller B, Bremmer F, Sahlmann CO, Hijazi S, Bouter C, Trojan L, et al. Alterations in androgen deprivation enhanced prostate-specific membrane antigen (PSMA) expression in prostate cancer cells as a target for diagnostics and therapy. *EJNMMI Res* 2015;5:66 [PubMed: 26576996]
24. Bychkov A, Vutrapongwatana U, Tepmongkol S, Keelawat S. PSMA expression by microvasculature of thyroid tumors - Potential implications for PSMA theranostics. *Sci Rep* 2017;7:5202 [PubMed: 28701709]
25. Chang SS, O’Keefe DS, Bacich DJ, Reuter VE, Heston WD, Gaudin PB. Prostate-specific membrane antigen is produced in tumor-associated neovasculature. *Clin Cancer Res* 1999;5:2674–81 [PubMed: 10537328]
26. Milowsky MI, Nanus DM, Kostakoglu L, Sheehan CE, Vallabhajosula S, Goldsmith SJ, et al. Vascular targeted therapy with anti-prostate-specific membrane antigen monoclonal antibody J591 in advanced solid tumors. *J Clin Oncol* 2007;25:540–7 [PubMed: 17290063]
27. Ben Jemaa A, Bouraoui Y, Oueslati R. Insight into the heterogeneity of prostate cancer through PSA-PSMA prostate clones: mechanisms and consequences. *Histol Histopathol* 2014;29:1263–80 [PubMed: 24788382]
28. Salas Fragomeni RA, Amir T, Sheikhabaei S, Harvey SC, Javadi MS, Solnes LB, et al. Imaging of Nonprostate Cancers Using PSMA-Targeted Radiotracers: Rationale, Current State of the Field, and a Call to Arms. *J Nucl Med* 2018;59:871–7 [PubMed: 29545375]
29. Backhaus P, Noto B, Avramovic N, Grubert LS, Huss S, Bögemann M, et al. Targeting PSMA by radioligands in non-prostate disease-current status and future perspectives. *Eur J Nucl Med Mol Imaging* 2018;45:860–77 [PubMed: 29335762]
30. Derlin T, Kreipe HH, Schumacher U, Soudah B. PSMA Expression in Tumor Neovasculature Endothelial Cells of Follicular Thyroid Adenoma as Identified by Molecular Imaging Using 68Ga-PSMA Ligand PET/CT. *Clin Nucl Med* 2017;42:e173–e4 [PubMed: 27997422]
31. Lapa C, Werner RA, Schmid JS, Papp L, Zsótér N, Biko J, et al. Prognostic value of positron emission tomography-assessed tumor heterogeneity in patients with thyroid cancer undergoing treatment with radiopeptide therapy. *Nucl Med Biol* 2015;42:349–54 [PubMed: 25595135]
32. Werner RA, Ilhan H, Lehner S, Papp L, Zsótér N, Schatka I, et al. Pre-therapy Somatostatin Receptor-Based Heterogeneity Predicts Overall Survival in Pancreatic Neuroendocrine Tumor Patients Undergoing Peptide Receptor Radionuclide Therapy. *Mol Imaging Biol* 2018
33. Bundschuh RA, Dinges J, Neumann L, Seyfried M, Zsótér N, Papp L, et al. Textural Parameters of Tumor Heterogeneity in ¹⁸F-FDG PET/CT for Therapy Response Assessment and Prognosis in Patients with Locally Advanced Rectal Cancer. *J Nucl Med* 2014;55:891–7 [PubMed: 24752672]
34. Yip SS, Aerts HJ. Applications and limitations of radiomics. *Phys Med Biol* 2016;61:R150–66 [PubMed: 27269645]
35. Rizzo S, Botta F, Raimondi S, Origgi D, Fanciullo C, Morganti AG, et al. Radiomics: the facts and the challenges of image analysis. *Eur Radiol Exp* 2018;2:36 [PubMed: 30426318]
36. Graf J, Pape UF, Jann H, Denecke T, Arsenic R, Brenner W, et al. Prognostic Significance of Somatostatin Receptor Heterogeneity in Progressive Neuroendocrine Tumor Treated with Lu-177 DOTATOC or Lu-177 DOTATATE. *Eur J Nucl Med Mol Imaging* 2019

37. Emmett L, Crumbaker M, Ho B, Willowson K, Eu P, Ratnayake L, et al. Results of a Prospective Phase 2 Pilot Trial of. *Clin Genitourin Cancer* 2019;17:15–22 [PubMed: 30425003]
38. Eberlein U, Cremonesi M, Lassmann M. Individualized Dosimetry for Theranostics: Necessary, Nice to Have, or Counterproductive? *J Nucl Med* 2017;58:97S–103S [PubMed: 28864620]
39. Flux GD, Sjøgreen Gleisner K, Chiesa C, Lassmann M, Chouin N, Gear J, et al. From fixed activities to personalized treatments in radionuclide therapy: lost in translation? *Eur J Nucl Med Mol Imaging* 2018;45:152–4 [PubMed: 29080096]
40. Lassmann M, Eberlein U. The Relevance of Dosimetry in Precision Medicine. *J Nucl Med* 2018;59:1494–9 [PubMed: 30002109]
41. Hänscheid H, Lapa C, Buck AK, Lassmann M, Werner RA. Dose Mapping After Endoradiotherapy with. *J Nucl Med* 2018;59:75–81 [PubMed: 28588150]
42. Begum NJ, Thieme A, Eberhardt N, Tauber R, D'Alessandria C, Beer AJ, et al. The Effect of Total Tumor Volume on the Biologically Effective Dose to Tumor and Kidneys for. *J Nucl Med* 2018;59:929–33 [PubMed: 29419479]
43. Kletting P, Kull T, Maaß C, Malik N, Luster M, Beer AJ, et al. Optimized Peptide Amount and Activity for ⁹⁰Y-Labeled DOTATATE Therapy. *J Nucl Med* 2016;57:503–8 [PubMed: 26678617]
44. Kletting P, Schuchardt C, Kulkarni HR, Shahinfar M, Singh A, Glatting G, et al. Investigating the Effect of Ligand Amount and Injected Therapeutic Activity: A Simulation Study for ¹⁷⁷Lu-Labeled PSMA-Targeting Peptides. *PLoS One* 2016;11:e0162303 [PubMed: 27611841]
45. Cazaente T, Morschhauser F, Vermandel M, Betrouni N, Prangère T, Steinling M, et al. Pre-therapy ¹⁸F-FDG PET quantitative parameters help in predicting the response to radioimmunotherapy in non-Hodgkin lymphoma. *Eur J Nucl Med Mol Imaging* 2010;37:494–504 [PubMed: 19820933]
46. Wang H, Shen G, Jiang C, Li L, Cui F, Tian R. Prognostic value of baseline, interim and end-of-treatment ¹⁸F-FDG PET/CT parameters in extranodal natural killer/T-cell lymphoma: A meta-analysis. *PLoS One* 2018;13:e0194435 [PubMed: 29558489]
47. Wang J, Zang J, Wang H, Liu Q, Li F, Lin Y, et al. Pretherapeutic ⁶⁸Ga-PSMA-617 PET May Indicate the Dosimetry of ¹⁷⁷Lu-PSMA-617 and ¹⁷⁷Lu-EB-PSMA-617 in Main Organs and Tumor Lesions. *Clin Nucl Med* 2019
48. Violet J, Jackson P, Ferdinandus J, Sandhu S, Akhurst T, Iravani A, et al. Dosimetry of ¹⁷⁷Lu-PSMA-617 in Metastatic Castration-Resistant Prostate Cancer: Correlations Between Pretherapeutic Imaging and Whole-Body Tumor Dosimetry with Treatment Outcomes. *J Nucl Med* 2019;60:517–23 [PubMed: 30291192]
49. Nedrow JR, Latoche JD, Day KE, Modi J, Ganguly T, Zeng D, et al. Targeting PSMA with a Cu-64 Labeled Phosphoramidate Inhibitor for PET/CT Imaging of Variant PSMA-Expressing Xenografts in Mouse Models of Prostate Cancer. *Mol Imaging Biol* 2016;18:402–10 [PubMed: 26552656]
50. Klug F, Prakash H, Huber PE, Seibel T, Bender N, Halama N, et al. Low-dose irradiation programs macrophage differentiation to an iNOS⁺/M1 phenotype that orchestrates effective T cell immunotherapy. *Cancer Cell* 2013;24:589–602 [PubMed: 24209604]

TRANSLATIONAL RELEVANCE

Radioligand therapy (RLT) targeting the prostate specific membrane antigen (PSMA) is an emerging treatment modality for advanced prostate cancer but 50% of patients with PSMA-positive tumors experience treatment failure. Here we demonstrate in mouse models of prostate cancer that low or heterogeneous tumor PSMA expression represents a resistance mechanism to ^{177}Lu - and ^{225}Ac -PSMA RLT. In tumors with different levels of PSMA expression/cell or varying fractions of PSMA-positive cells, PSMA expression correlated with radioligand uptake and DNA damage and, thus, RLT efficacy. Intra- and inter-lesion variations in PSMA might result in undertreatment which reduces RLT efficacy and may select treatment resistant tumor clones. Systematic assessment of intra- and inter-lesion PSMA heterogeneity is currently not feasible clinically; however, this issue might be addressed by individual patient dosimetry to optimize safely delivered maximal tumor doses.

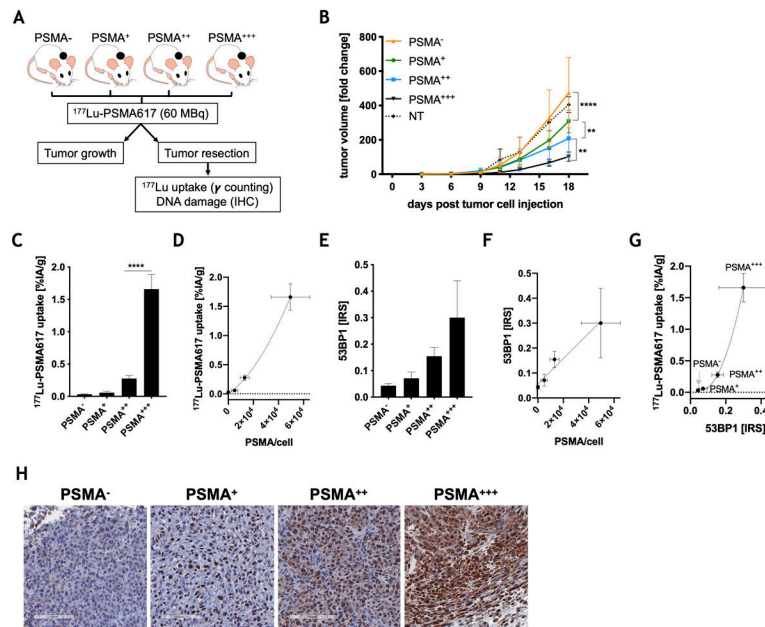


Figure 1. PSMA levels/cell translate into RLT efficacy.

(A) Experimental design of study 1. (B) Mean \pm SD of the relative tumor growth following PSMA-RLT (compared to pre-treatment tumor volume) is shown (n=9 mice/group, PSMA⁺⁺⁺>PSMA⁺⁺, p=0.0015; PSMA⁺⁺>PSMA⁺, p=0.0016; PSMA⁺>PSMA⁻, p<0.0001; PSMA⁻, RLT vs. NT, p=0.3517). For visibility reasons, the depiction of untreated controls is limited to that of PSMA⁻ tumors (compare Supplementary Figure S1C). (C-H) In a subset of mice (n=3 tumors/group), tumors were resected two days after RLT. (C) ¹⁷⁷Lu-PSMA617 uptake in RM1 sublines (PSMA⁺⁺ vs. PSMA⁺⁺⁺, p<0.0001; PSMA⁺ vs. PSMA⁺⁺, p=0.0959; PSMA⁻ vs. PSMA⁺, p=0.7789). (D) PSMA cell surface expression (flow cytometry) determines ¹⁷⁷Lu-PSMA tumor uptake (R²=0.9797). (E) Quantification of 53BP1 foci across groups (PSMA⁺⁺ vs. PSMA⁺⁺⁺, p=0.1473; PSMA⁺ vs. PSMA⁺⁺, p=0.3563; PSMA⁻ vs. PSMA⁺, p=0.6483). (F) Association of PSMA cell surface expression (flow cytometry) with DNA damage. (linear regression, R²=0.7154). (G) Correlation of 53BP1 foci with ¹⁷⁷Lu-PSMA uptake (R²=0.9803). (H) Representative IHC images. Brown staining represents 53BP1 positivity. Graphs represent mean \pm SD. Asterisks indicate statistical significance.

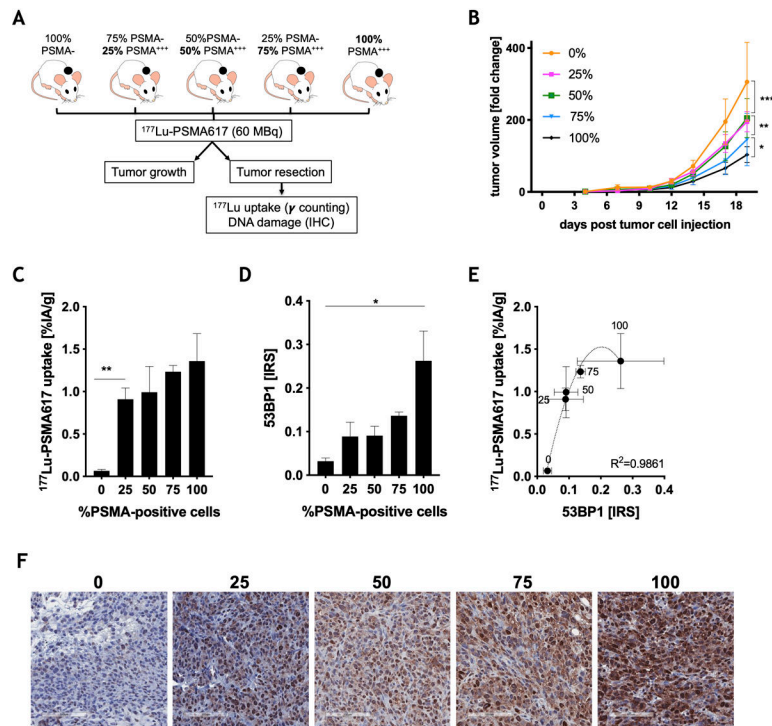


Figure 2. Intra-tumor PSMA heterogeneity determines treatment response.

(A) Experimental design. (B) The mean \pm SD of the relative tumor growth following PSMA-RLT (compared to pre-treatment tumor volume) is shown (n=7 mice/group; 100% vs. 75%, p=0.0177; 75% vs. 50%, p=0.0012; 50% vs. 25%, p=0.5492; 25% vs. 0%, p<0.0001). (C-F) Tumors (n=3 tumors/group) were resected two days after RLT. (C) ^{177}Lu -PSMA617 uptake in the different experimental groups ($R^2=0.9398$; 100% vs. 75%, p=0.7318; 75% vs. 50%, p=0.4701; 50% vs. 25%, p=0.7318; 25% vs. 0%, p=0.0042). (D) Quantification of 53BP1 foci across groups ($R^2=0.9372$; 100% vs. 75%, p=0.3330; 75% vs. 50%, p=0.9036; 50% vs. 25%, p=0.9787; 25% vs. 0%, p=0.9036). (E) Relationship between 53BP1 foci and ^{177}Lu -PSMA617 uptake ($R^2=0.9861$). (F) Representative IHC images. Brown staining indicates 53BP1 positivity. Graphs represent mean \pm SD. Asterisks indicate statistical significance. The numbers 0, 25, 50, 75, 100 indicate the percentage of PSMA-positive cells injected (vs. PSMA-negative cells).

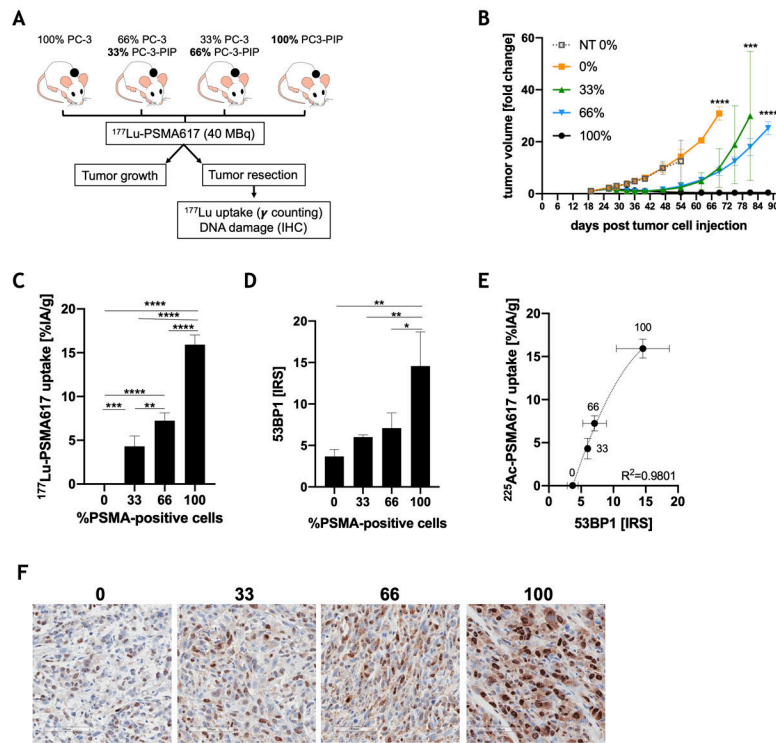


Figure 3. Intra-tumor PSMA heterogeneity determines treatment response in a human PC model.

(A) Experimental design. (B) The mean \pm SD of the relative tumor growth following PSMA-RLT (compared to pre-treatment tumor volume) is shown ($n=7$ mice/group, data were plotted for group sizes 3; 100% vs. 66%, $p<0.0001$; 66% vs. 33%, $p=0.0001$; 33% vs. 0%, $p<0.0001$). For visibility reasons, the depiction of untreated controls is limited to that of PSMA- tumors (compare Supplementary Figure S5C). (C-F) Tumors ($n=3$ tumors/group) were resected two days after RLT. (C) ^{177}Lu -PSMA617 uptake in the different experimental groups ($R^2=0.9827$; 100% vs. 66%, $p<0.0001$; 66% vs. 33%, $p=0.0046$; 33% vs. 0%, $p=0.0009$). (D) Quantification of 53BP1 foci across groups ($R^2=0.7910$; 100% vs. 66%, $p=0.0159$; 66% vs. 33%, $p=0.5838$; 33% vs. 0%, $p=0.4323$). (E) Relationship between 53BP1 foci and ^{177}Lu -PSMA617 uptake ($R^2=0.9801$). (F) Representative IHC images. Brown staining indicates 53BP1 positivity. Mean \pm SD are shown (B-E). Asterisks indicate statistical significance. The numbers 0, 33, 66, 100 indicate the percentage of PC-3-PIP (PSMA $^{+++}$) cells injected (vs. PSMA-negative PC-3).

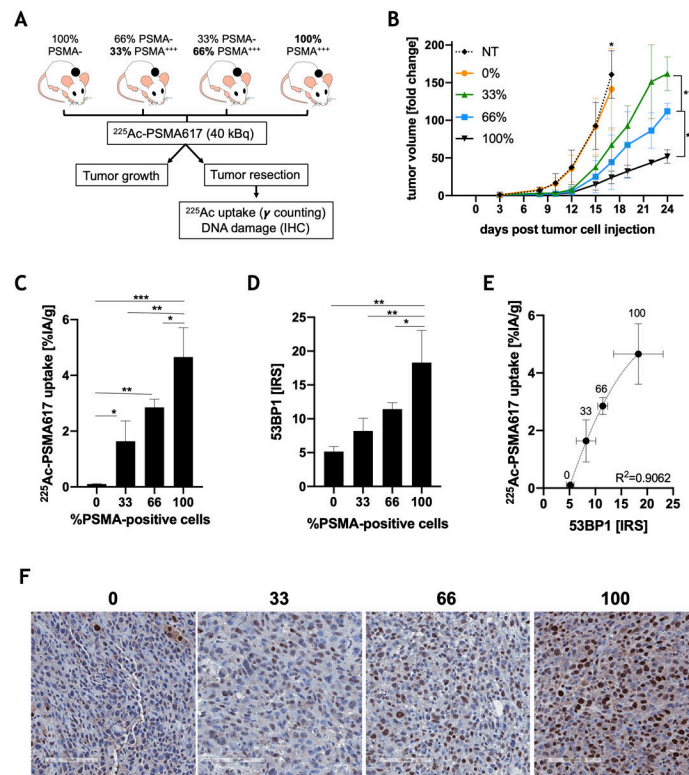


Figure 4. Efficacy of ^{225}Ac -PSMA in tumors with heterogeneous PSMA expression.

(A) Experimental design. (B) The mean \pm SD of the relative tumor growth following PSMA-RLT (compared to pre-treatment tumor volume) is shown ($n=7$ mice/group; 100% vs. 66%, $p=0.0020$; 66% vs. 33%, $p=0.0028$; 33% vs. 0%, on day 17, $p=0.0120$). For visibility reasons, the depiction of untreated controls is limited to that of PSMA- tumors (compare Supplementary Figure S6D). (C-F) Tumors ($n=3$ tumors/group) were resected two days after RLT. (C) ^{225}Ac -PSMA617 uptake in the different experimental groups ($R^2=0.9967$; 100% vs. 66%, $p=0.0291$; 66% vs. 33%, $p=0.0532$; 33% vs. 0%, $p=0.0416$). (D) Quantification of 53BP1 foci across groups ($R^2=0.8329$; 100% vs. 66%, $p=0.0497$; 66% vs. 33%, $p=0.3142$; 33% vs. 0%, $p=0.3142$). (E) Relationship between 53BP1 foci and ^{225}Ac -PSMA617 uptake ($R^2=0.9062$). (F) Representative IHC images. Brown staining indicates 53BP1 positivity. Graphs represent mean \pm SD. Asterisks indicate statistical significance. The numbers 0, 33, 66, 100 indicate the percentage of PSMA-positive RM1 cells injected (vs. PSMA-negative cells).